BMC Gastroenterology

RESEARCH

Open Access

Evaluating the diagnostic significance of the R2* value on 3.0T MRI for assessing the severity of warm hepatic ischemia-reperfusion injury

Shichao Xu[1*], Qian Ji[2] and Jing Xu[1]

Abstract

Background Magnetic resonance imaging (MRI) may be a non-invasive tool for managing warm hepatic ischemia-reperfusion injury (WHIRI).

Purpose We aimed to evaluate the diagnostic utility of the R2* values derived from 3.0T blood oxygen level-dependent (BOLD) MRI in assessing the severity of WHIRI.

Methods Fifty healthy adult New Zealand white rabbits were randomly divided into 5 groups with 10 rabbits in each. The experimental groups (40 rabbits) underwent clamping of the hepatic artery and the portal vein for 10, 20, 30, or 40 min, followed by 6 h of reperfusion to induce WHIRI. The other 10 rabbits comprised the normal control group. All animals were underwent conventional 3.0 T and BOLD MRI. Animals were euthanized and the serum levels of biochemical indicators were determined. Correlations between R2* values, biochemical indicators, and WHIRI staging were assessed using Spearman's rank correlation coefficient. The diagnostic efficacy of R2* values was evaluated using ROC curves.

Results R2* values increased gradually with prolonged warm ischemia with significant differences across groups ($F = 133.25$, $P < 0.05$). A strong positive correlation was detected between R2* values and WHIRI staging ($r = 0.878$, $P = 0.000$). Biochemical indicators (ALT, AST, LDH, MDA, and MPO) increased significantly, while SOD levels decreased with prolonged warm ischemia ($P < 0.05$). R2* values exhibited a strong positive correlation with biochemical indicators ($r > 0.495$) and a negative correlation with SOD levels (r=-0.658). The diagnostic efficacy of the R2* values was highest for predicting WHIRI above stage S4 (AUC = 1.000).

Conclusion R2* values on BOLD MRI provide a sensitive and accurate method for assessing WHIRI. The diagnostic efficacy of the R2* values was the best for predicting WHIRI above stage S4.

Keywords Hepatic warm ischemia-reperfusion injury, BOLD MRI, R2* value, Biochemical indicators, Diagnostic efficacy

*Correspondence:
Shichao Xu
xushichao354@163.com

[1]Department of General Surgery, Tianjin Union Medical Center, The First Affiliated Hospital of Nankai University, No.190 Jieyuan Road, Hongqiao District, Tianjin City 300121, China
[2]Department of Radiology, Tianjin First Central Hospital, Tianjin City 300192, China

Introduction

Hepatectomy remains the primary treatment for both benign and malignant liver lesions due to unique liver anatomy and the dual blood supply from the portal vein and hepatic artery. Warm hepatic ischemia-reperfusion injury (WHIRI) occurs when tissues and organs with prolonged warm ischemia and anoxia regain the blood supply, which aggravates rather than alleviates the injury [1]. WHIRI leads to pathologic processes, including organ dysfunction, structural damage, and cell death. As a complex pathophysiologic process, WHIRI commonly complicates various surgical procedures involving the liver, such as hemorrhagic shock, liver trauma, hepatectomy, and liver transplantation [1, 2]. WHIRI is a significant concern in surgery due to the damage caused by prolonged ischemia followed by reperfusion [1, 2]. This complication often arises in various hepatic surgical procedures and can result in liver failure and dysfunction, impacting patient outcomes [1, 2].

Magnetic resonance imaging (MRI) has become instrumental in abdominal organ evaluation due to its non-invasive nature and high resolution.[3] Recent studies have explored the use of multiparametric MRI techniques, including blood oxygenation level-dependent (BOLD) MRI, diffusion tensor imaging (DTI), and intravoxel incoherent motion (IVIM) MRI, to assess hepatic responses to injury and treatment strategies [3–6].

For example, Lipo-PGE1 treatment has shown potential in protecting against hepatic warm ischemia-reperfusion injury (WIRI) [4]. Studies utilizing multiparametric MRI in animal models have highlighted the effectiveness of prophylactic Lipo-PGE1 pretreatment approaches [4]. Furthermore, IVIM, DTI, and BOLD MRI have been investigated for the ability to evaluate hepatic pathophysiologic changes, providing insight into associated microenvironmental alterations [4–6]. Additionally, research has focused on the diagnostic value of specific MRI parameters, such as the R2* values on BOLD MRI, in combination with serum biochemical indicators to aid in the early detection and assessment of hepatic WHIRI [5, 6]. These studies emphasize the potential of multiparametric MRI as a non-invasive tool for monitoring the therapeutic intervention impact on hepatic WIRI [5, 6].

The objective of the current study was to further investigate the diagnostic utility of MRI-derived parameters, particularly R2* values on BOLD MRI, along with serum biochemical indicators for the early detection and assessment of hepatic WHIRI. Additionally, pathologic examinations of liver tissues will be performed to assess the diagnostic value of MRI-derived parameters in identifying hepatic injury and evaluating treatment efficacy. Through this research, we aim to enhance our understanding of hepatic WHIRI mechanisms and improve clinical management strategies.

Materials and methods

Animal model construction and grouping

The experiments were conducted in accordance with the *National Guidelines for the Administration of Experimental Animals* and was approved by the Ethical Committee.

Fifty healthy adult New Zealand white rabbits (Tianjin Laboratory Animal Center, Tianjin, China), weighing 2.5–3.0 kg, were randomly divided into the following 5 groups with 10 rabbits in each group: normal control group (N0 group), and 4 experimental groups undergoing warm ischemia for 10 min (T10 group), 20 min (T20 group), 30 min (T30 group), and 40 min (T40 group). The animals were subjected to a 4-h fast and were deprived of water for 4 h before the experiment. Next, the animals were weighed. The weight of the rabbits was maintained at 2.5–3.0 kg before the experiments. Rabbits that did not meet the weight range criterion were excluded. No rabbits were excluded at this stage.

(1) Construction of the rabbit model of WHIRI: The rabbits received intravenous anesthesia with 5% pentobarbital at a dose of 1 ml/kg via the marginal ear vein. Following successful administration of anesthesia at room temperature (25℃), the rabbits' abdomens were dehaired and a midline abdominal incision was made below the xiphoid process. The abdominal wall was dissected layer-by-layer to access the peritoneal cavity. The Pringle maneuver was performed to expose the hepatoduodenal ligament. An atraumatic vascular clamp was applied to the hepatoduodenal ligament to induce warm ischemia. Real-time intraoperative physiologic signal monitoring of the liver was performed using the MP150 model 16-channel multichannel physiologic recorder (Biopac Systems, Inc.,Washington, USA) to confirm the success of the vascular clamping. A probe inserted into the liver parenchyma recorded the blood flow changes before and during vascular clamping and after blood supply recovery. The incision was covered with sterile saline gauze to maintain peritoneal cavity hydration. Portal venous and hepatic arterial blood supply were obstructed for 10, 20, 30, or 40 min, after which the vascular clamp was removed to restore the blood supply. The peritoneal cavity was closed.

(2) Normal control group: No surgery was performed in this group and the animals underwent clinical laboratory tests immediately after anesthesia. The severity of WHIRI was defined in the normal control and experimental groups subjected to 0, 10, 20, 30, or 40 min of warm ischemia was defined as stages S0, S1, S2, S3, and S4, respectively.

MRI machine and scan parameters

The animals received intramuscular anesthesia with Lumianning (0.1 ml/kg; Jilin Huamu Animal Health Products Co., Ltd., Jilin province, China) 5–10 min at 6 h after

the model construction. Then the rabbits were immobilized on the MRI scanning bed in the supine position. MRI scans were performed using a Siemens Magnetom Trio 3.0T MRI machine (Siemens AG, Munich, Germany). A 32-channel phased-array body coil was used and a sandbag was placed on the abdomen to suppress respiratory motion. The coil center was positioned over the liver. Scan sequences and parameters were as follows: t1) Transverse T1-weighted imaging was used for conventional MR scan, spin-echo (SE) sequence for T2WI, and fast spin echo (FSE) sequence for coronal T2WI; and (2) gradient recalled echo (GRE) sequence was used for BOLD MRI in the transverse plane with a reception time of 75 ms using 9 echo time values (2.57, 5.23, 7.52, 9.81, 12.10, 14.39, 16.68, 18.97, and 24.25 ms). Other parameters were as follows: slice thickness, 3 mm; slice interval, 0.3 mm; field of view, 200 mm×200 mm; bandwidth, 62.5 Hz; matrix, 128 × 128; and number of excitations, 1.

Image measurement and analysis

The raw images and pseudo-color images of T2* were generated automatically after BOLD imaging. The raw T2* MRI images were analyzed using ImageJ (v1.43b; National Institutes of Health, Bethesda, MD, USA) to obtain R2* MRI images. An imaging specialist with at least 3 years of working experience delineated the region-of-interest (ROI). ROIs were selected on three image layers encompassing the liver center, referencing T2WI images on the same layers and avoiding large vessels in the liver parenchyma and gallbladder and its edges. Two circular ROIs were selected in the left and right lobes of the liver and the T2* values were measured on the pseudo-color images of T2* and averaged. The R2* value was calculated according to the following formula: R2*=1/T2*.

Histologic and biochemical examinations

(1) Liver function test: Liver function indicators, including aspartate aminotransferase (AST), alanine aminotransferase (ALT), and lactate dehydrogenase (LDH), were recorded. Blood was collected from the marginal ear vein after the 3.0T MRI and the liver function indicators were detected using a fully automatic biochemical analyzer (Hitachi TAB-40F2; Tokyo, Japan).

(2) Superoxide dismutase (SOD), malondialdehyde (MDA), and myeloperoxidase (MPO) in liver tissues: The levels of SOD, MDA, and MPO were measured using the enzymatic reaction principles and a spectrophotometer. The SOD, MDA, and MPO detection kits were purchased from Nanjing Jiancheng Bioengineering Research Institute (Nanjing, China).

(3) The rabbits received intravenous anesthesia with 5% pentobarbital at a dose of 1 ml/kg via the marginal ear vein for euthanasia. Then the rabbits were euthanized by air embolization and the liver tissues were harvested after opening the abdomen. After removing the liver capsule, the liver tissues were cut into l cm^3 blocks and fixed in 10% formaldehyde solution for > 24 h. The tissues were embedded in paraffin, sequentially sectioned at a thickness of 5 μm, and subjected to conventional hematoxylin and eosin (HE) staining. Pathologic and micromorphologic changes of the liver tissues were observed under a light microscope (Olympus BX50, Tokyo, Japan).

Statistical analysis

All data were analyzed using SPSS 17.0 software. Measurements are expressed as the mean ± standard deviation. The mean R2* values were compared across the WHIRI stages using one-way ANOVA. Intergroup pairwise comparisons were performed using the Dunnett T_3 test. The distribution of animals at different stages of WHIRI was compared across the groups using the non-parametric Mann-Whitney U test. The differences in biochemical indicators were compared between the groups using the non-parametric Kruskal-Wallis test. The correlations between the R2* values, biochemical indicators, and staging of WHIRI were examined using the non-parametric Spearman test. The diagnostic efficacy of the mean R2* values was assessed by plotting the receiver operating characteristic (ROC) curve. The cut-off value with the largest Yoden index was defined and specificity and sensitivity were calculated accordingly. A correlation coefficient (r) > 0.5 was considered a good strength of the relationship, and a $P < 0.05$ were considered statistically significant.

Results

Distributions and variations of R2* values across the groups

R2* images revealed lower T2* signal intensity in the liver in the experimental groups compared to the control group, which gradually decreased as the duration of warm ischemia increased (Fig. 1). The apparent spin-spin relaxation rate (R2*) was estimated from the slope of the logarithmic signal intensity curve of T2* using the following formula: R2*=1/T2*. The mean R2* values differed significantly across the groups with values of 105.96 ± 10.09 Hz in the control group and 126.01 ± 5.02 Hz, 127.40 ± 8.75 Hz, 136.97 ± 7.06 Hz, and 183.44 ± 7.66 Hz in the experimental groups subjected to warm ischemia for 10, 20, 30, and 40 min, respectively ($F = 133.25$, $P < 0.05$). However, there were no significant differences in mean R2* values between the experimental

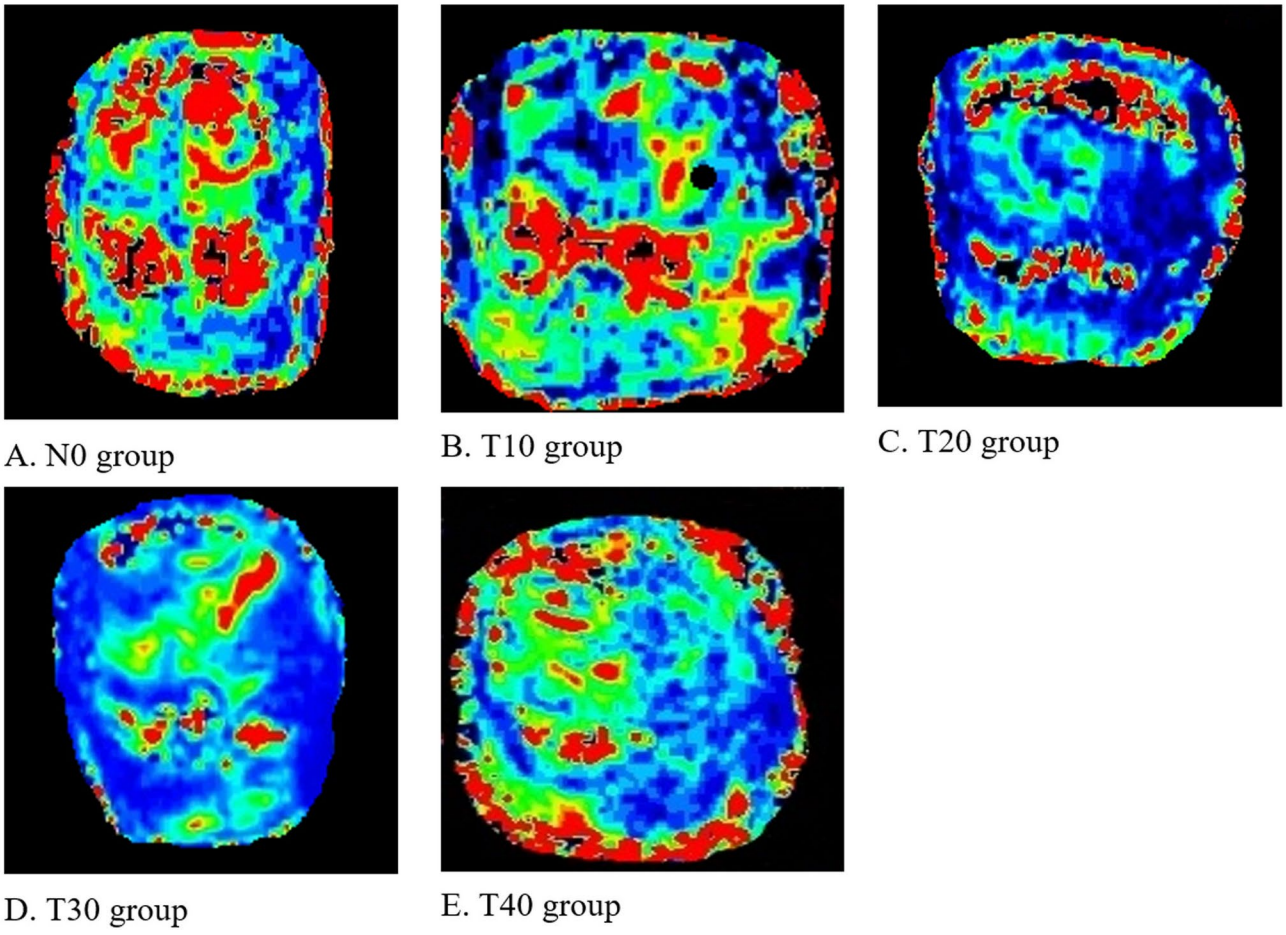

Fig. 1 Pseudo-color images of MRI liver R2* in experimental groups. **(A)** N0 group; **(B)** T10 group; **(C)** T20 group; **(D)** T30 group; **(E)** T40 group

Table 1 Comparisons of R2* values at different stages using the Mann-Whitney U test

Staging of WHIRI	Cases	Mean R2*	Z	*P*
S0	10	105.96 ± 10.09	-4.535	< 0.001
≥S1	40	143.46 ± 24.77		
≤S1	20	115.99 ± 12.88	-4.673	< 0.001
≥S2	30	149.27 ± 26.02		
≤S2	30	119.79 ± 12.75	-5.406	< 0.001
≥S3	20	160.21 ± 24.89		
≤S3	40	124.09 ± 13.75	-4.851	< 0.001
S4	10	183.44 ± 7.66		

Notes: The severity of WHIRI was defined in the normal control and experimental groups subjected to 10, 20, 30, or 40 min of warm ischemia was defined as stages S0, S1, S2, S3, and S4, respectively

groups receiving warm ischemia for 10 and 20 min or between the groups receiving warm ischemia for 20 and 30 min ($P > 0.05$). Significant differences were detected between other pairs of groups ($P < 0.05$). The mean R2* values at different stages of WHIRI are shown in Table 1. The mean R2* value significantly increased as warm ischemia increased (Fig. 2, $P = 0.000$). A strong positive correlation was detected between the mean R2* values and WHIRI staging ($r = 0.878$, $P = 0.000$), which indicated an increase in the mean R2* value with worsening WHIRI severity.

Variations of biochemical indicators and correlations to R2* values

After 6 h of reperfusion, the serum levels of ALT, AST, and LDH were significantly higher in the experimental groups compared to the control group. The serum levels of ALT, AST, and LDH increased as the warm ischemia increased. Similarly, the MDA and MPO levels in liver tissues in the experimental groups were significantly higher than the control group, which further increased as warm ischemia duration increased. The total SOD level in liver tissues was consistently low in the experimental groups with a decreasing trend as warm ischemia increased. All biochemical indicators showed significant differences between groups ($P < 0.05$; Table 2). Spearman's rank correlation coefficient showed a strong positive correlation between the mean R2* values and the levels of ALT, AST, LDH, MPO, and MDA ($r > 0.495$, $P < 0.05$), and a strong

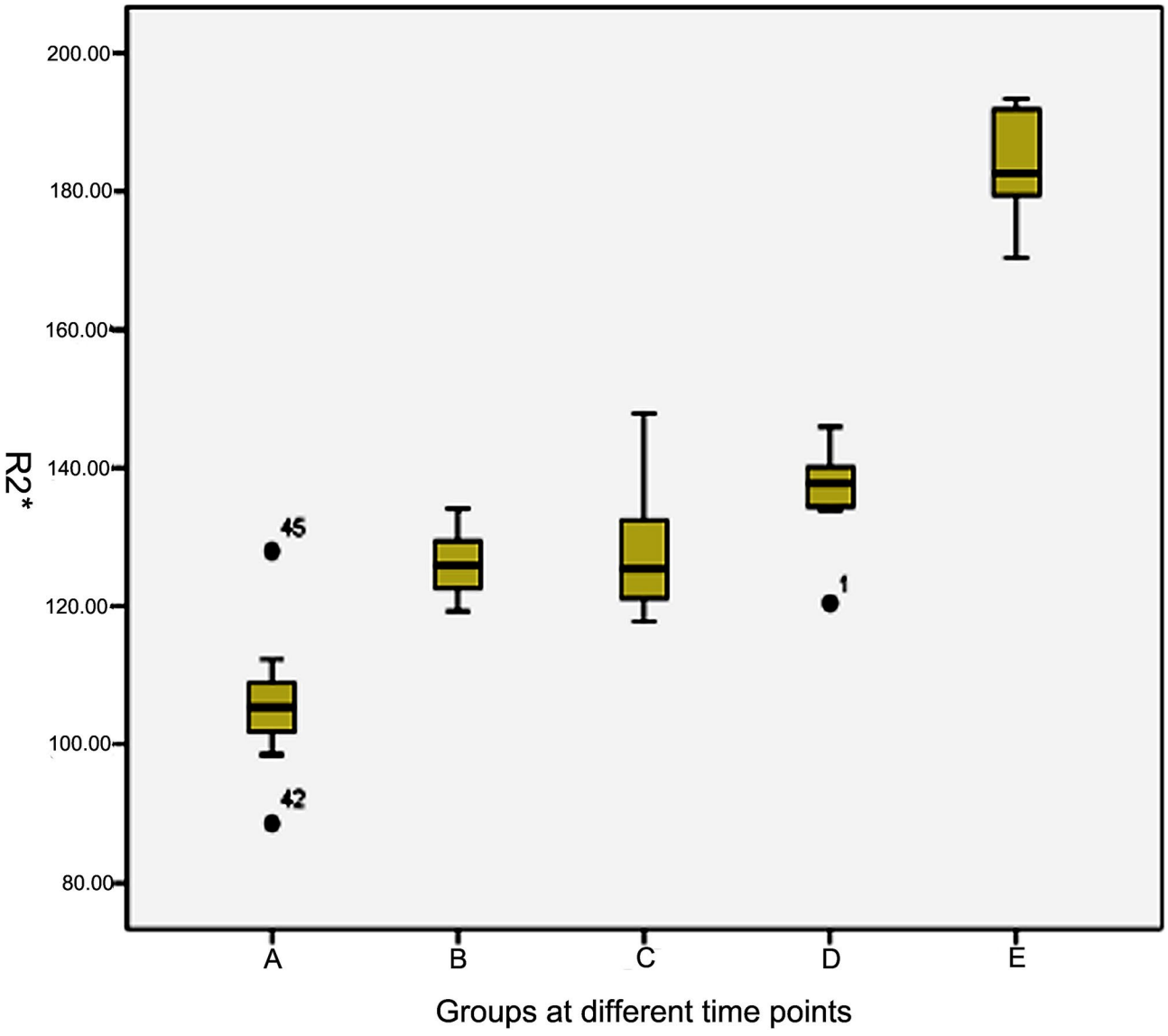

Fig. 2 Boxplots of R2* values in each group at different timepoints (**A**: control group; **B**: Group receiving warm ischemia for 10 min; **C**: Group receiving warm ischemia for 20 min; **D**: Group receiving warm ischemia for 30 min; **E**: Group receiving warm ischemia for 40 min. The data of boxplots are presented as medians, quartiles and Max/Min values

Table 2 Comparison of median biochemical indicators in different groups using the Kruskal-Wallis test

Group	ALT(U/L)	AST(U/L)	LDH(U/L)	MDA(nmol/ml)	MPO (nkat/g)	SOD(U/ml)
Control group	34.50 (24.75 ~ 37.00)	36.00 (16.75 ~ 73.50)	225.50 (119.25 ~ 477.00)	2.07 (1.80 ~ 2.33)	13.72 (11.00 ~ 16.82)	174.59 (166.10 ~ 210.09)
10 min	47.50 (40.00 ~ 76.00)	106.50 (83.00 ~ 147.00)	464.50 (271.25 ~ 1335.25)	2.86 (2.50 ~ 3.19)	15.27 (13.27 ~ 17.03)	146.75 (139.43 ~ 154.89)
20 min	83.00 (54.25 ~ 137.50)	377.50 (240.25 ~ 758.75)	511.00 (405.00 ~ 919.50)	3.13 (2.81 ~ 3.38)	17.70 (17.15 ~ 22.68)	140.97 (128.90 ~ 154.35)
30 min	165.00 (65.00 ~ 247.75)	348.00 (297.75 ~ 708.25)	1117.00 (789.25 ~ 2024.75)	3.56 (3.07 ~ 3.77)	19.69 (16.70 ~ 21.35)	124.22 (109.91 ~ 129.13)
40 min	499.50 (144.75 ~ 1469.50)	738.50 (376.25 ~ 1082.75)	1458.50 (557.50 ~ 3423.00)	3.41 (3.22 ~ 3.76)	27.09 (21.68 ~ 31.31)	120.62 (110.69 ~ 128.13)
χ2	27.12	33.78	19.92	28.84	29.68	34.76
P value	0.000	0.000	0.001	0.000	0.000	0.000

Table 3 Results of correlation analysis between mean R2* and biochemical indicators

Statistics	ALT	AST	LDH	MDA	MPO	SOD
r	0.613	0.697	0.495	0.618	0.732	-0.658
P value	0.000	0.000	0.000	0.000	0.000	0.000

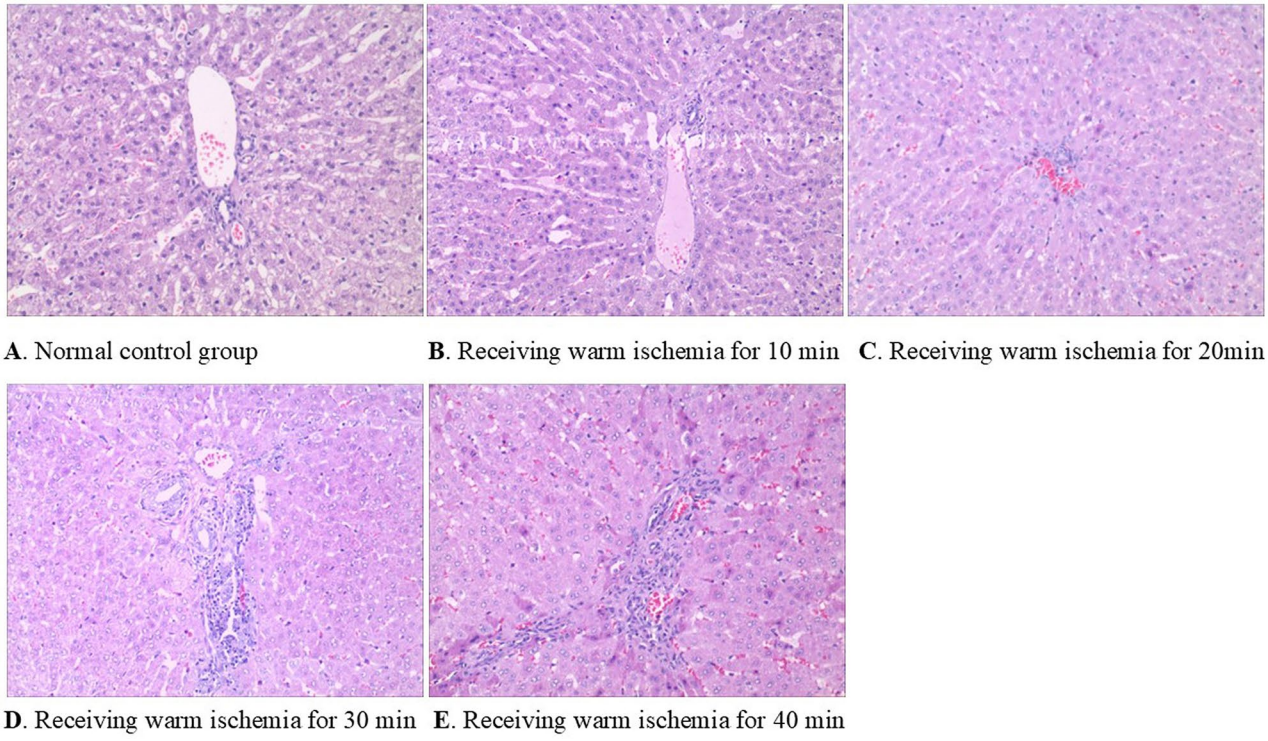

Fig. 3 HE staining of liver tissues in the experimental groups (×100 magnification). **(A)** Normal control group; **(B)** Receiving warm ischemia for 10 min; **(C)** Receiving warm ischemia for 20 min; **(D)** Receiving warm ischemia for 30 min; **(E)** Receiving warm ischemia for 40 min

Table 4 Diagnostic efficacy of the R2* value for predicting hepatic WHIRI above different stages

	AUC	Threshold of R2* value	Sensitivity	Specificity
Predicting hepatic WHIRI above stage S1	0.967	115.00	1.000	0.900
Predicting hepatic WHIRI above stage S2	0.893	132.00	0.733	0.950
Predicting hepatic WHIRI above stage S3	0.955	133.35	0.950	0.933
Predicting hepatic WHIRI above stage S4	1.000	159.05	1.000	1.000

negative correlation with the SOD level in liver tissues (r=-0.663, P = 0.001; Table 3).

Pathologic and micro-morphologic changes of liver tissues with prolongation of WHIRI

Liver sinusoids were neatly aligned in the control group with normal hepatocytes and absence of congestion or edema under light microscopy. Mild hepatocyte edema was observed after warm ischemia for 10 and 20 min with no significant dilatation or congestion of central veins sinusoids. However, diffuse hepatocyte swelling and distortion obviously occurred after 30 and 40 min of warm ischemia, accompanied by focal eosinophil-related necrosis and inflammatory cell infiltration in portal areas and hepatic lobules (Fig. 3).

Diagnostic efficacy of R2* values for WHIRI

The mean R2* values showed a significant increase in prolonged warm ischemia with high diagnostic efficacy in differentiating the WHIRI absence from any WHIRI stage (Table 4). The largest area under the ROC curve (AUC) was observed for the R2* value predicting WHIRI above stage S4 (1.000). The Yoden Index was 1.000, with a threshold of 159.05 Hz and sensitivity and specificity of 100%.

Discussion

In the current study the diagnostic utility of R2* values derived from BOLD MRI in assessing the severity of WHIRI was investigated. In 1990 Ogawa et al. [7] proposed the concept of the BOLD effect using gradient-echo sequences in high-strength magnetic fields

to highlight the para-magnetism of deoxyhemoglobin. BOLD MRI utilizes changes in the tissue oxygenation level, which in turn reflect alterations in local oxygen perfusion and metabolic oxygen consumption [8]. As warm ischemia persists, exacerbating liver hypoxia and microcirculatory dysfunction, the oxygen level in liver parenchyma decreases, leading to an increase in paramagnetic deoxyhemoglobin and subsequent changes in local magnetic sensitivity. Consequently, the signal intensity decreases on T2*-weighted imaging, resulting in an increase in the mean R2* value. The results revealed a significant increase in the mean R2* values with prolonged warm ischemia, which are consistent with previous studies [5, 6]. This finding aligns with the concept proposed by Ogawa et al. [7, 8] in 1990, highlighting the BOLD effect as a marker for tissue oxygenation levels.

The liver is susceptible to ischemia and hypoxia exacerbates WHIRI, which is characterized by hepatocellular damage, inflammatory cell infiltration, and liver function impairment [9]. In the current study, the serum levels of ALT, AST, and LDH along with the tissue levels of MDA and MPO were significantly elevated in experimental groups compared to controls with further increases observed with prolonged warm ischemia [10]. The MPO activity of liver tissues was determined as a measure of neutrophil infiltration and inflammatory response [11, 12]. In contrast, the total SOD levels decreased progressively with prolonged warm ischemia [11–13]. These findings suggest a correlation between biochemical indicators and WHIRI severity, with ALT, AST, LDH, MDA, and MPO positively correlated with WHIRI severity and SOD negatively correlated with WHIRI severity. We observed significant correlations between mean R2* values and key biochemical indicators of liver injury, including ALT, AST, LDH, MPO, MDA, and SOD, corroborating previous findings [7]. These correlations suggest that R2* values may serve as a surrogate marker for WHIRI severity, in agreement with previous studies emphasizing the relationship between MRI-derived parameters and biochemical/histopathologic parameters [5, 6, 9–13].

Although biochemical indicators provide valuable insights into liver damage, biochemical indicators lack specificity for diagnosing WHIRI and should be used in conjunction with the mean R2* value for diagnostic purposes. The correlation analysis demonstrated a positive correlation between the mean R2* value and biochemical indicators, further supporting the utility of the R2* value in the WHIRI diagnosis. The high diagnostic efficacy of the R2* value across all WHIRI stages underscores its potential as a diagnostic tool, particularly in distinguishing between the presence and absence of WHIRI and differentiating severity levels. Notably, the R2* value exhibited the highest diagnostic efficacy for WHIRI induced by prolonged warm ischemia, which aligned with previous studies suggesting a safety duration limit of 30 min for complete hepatic blood supply obstruction [14]. The diagnostic utility of R2* values in WHIRI assessment has significant implications for clinical practice, consistent with previous research highlighting the potential of multiparametric MRI as a non-invasive radiologic evaluation tool [5, 6, 14]. By providing quantitative measures of tissue oxygenation levels, R2* values offer valuable insight into WHIRI pathophysiology and may aid in prognostic assessment and treatment planning for patients undergoing liver surgery.

Despite these findings, the present study had limitations. BOLD signal intensity changes depend not only on local oxygenation but also on blood perfusion [15]. Thus, combining BOLD MRI with perfusion imaging techniques, such as CT perfusion, arterial spin labeling, and intravoxel incoherent motion, may provide more comprehensive assessment of WHIRI. Moreover, the study was limited to animal experiments, warranting further in vivo and clinical validation [16, 17]. Future research should focus on validating these findings in clinical settings and exploring the potential of combining BOLD MRI with perfusion imaging techniques for a more comprehensive assessment of WHIRI pathophysiology.

In conclusion, the current study builds upon previous research by highlighting the diagnostic utility of R2* values derived from BOLD MRI in assessing the severity of hepatic WHIRI. The diagnostic efficacy of the R2* values was the best for predicting WHIRI above stage S4 with an AUC of 1.0 followed by both sensitivity and specificity of 100%. Further research incorporating advanced imaging techniques and clinical studies is warranted to validate these findings and translate the findings into clinical practice.

Abbreviations

WHIRI	Warm hepatic ischemia-reperfusion injury
MRI	Magnetic resonance imaging
BOLD	Blood oxygen level-dependent
DTI	Diffusion tensor imaging
IVIM	Intravoxel incoherent motion
WIRI	Warm ischemia-reperfusion injury
SE	Spin-echo
FSE	Fast spin echo
GRE	Gradient recalled echo
ROI	Region-of-interest
AST	Aspartate aminotransferase
ALT	Alanine aminotransferase
SOD	Superoxide dismutase
MDA	Malondialdehyde
MPO	Myeloperoxidase
HE	Hematoxylin and eosin
ROC	Receiver operating characteristic
AUC	Area under the ROC curve

Acknowledgements
Not applicable.

Author contributions
Concept - S.X., Q.J., J.X.; Design- S.X., Q.J., J.X.; Supervision - S.X.; Fundings - S.X.; Materials - S.X., Q.J., J.X.; Data Collection - S.X., Q.J., J.X.; Analysis and/or Interpretation - S.X., Q.J., J.X.; Writing - S.X., Q.J., J.X.; Critical Review - S.X., Q.J., J.X.

Funding
This study was supported by Tianjin Medical Key Discipline (Specialty) Construction Project (TJYXZDXK-058B), Tianjin Municipal Health Commission Key Research of Integrated Traditional Chinese and Western Medicine(2023056), Scientific Research Project of Tianjin Union Medical Center (2024YJ008), Beijing Science and Technology Innovation Medical Development Foundation (KC2021-JX-0186-93), Tianjin Key Medical Discipline (Specialty) Construction Project (No. TJYXZDXK-041 A), the Natural Science Foundation of Tianjin, China (No. 21JCYBJC01050), National Natural Science Foundation of China (NO. 81301197).

Data availability
The datasets used and/or analyzed during the current study are available from the corresponding author on reasonable request.

Declarations

Ethics approval and consent to participate
The sudy was conducted in accordance with the *National Guidelines for the Administration of Experimental Animals* and was approved by the Ethical Committee of the Experimental Animal Welfare Ethics Review Committee of Nankai University (No. 2023-SYDWLL-000158; approval date, 2023-2-23).

Consent for publication
Not applicable.

Competing interests
The authors declare no competing interests.

Received: 12 September 2024 / Accepted: 28 April 2025
Published online: 12 May 2025

References

1. Jiménez-Castro MB, Cornide-Petronio ME, Gracia-Sancho J, et al. Inflammasome-Mediated inflammation in liver Ischemia-Reperfusion injury. Cells. 2019;8:1131.
2. Specialized Committee of hepatobiliary and pancreatic Surgery, the Chinese Research Hospital Association. Chinese expert consensus on laparoscopic hepatectomy for hepatocellular carcinoma (2020 Edition). Chin J Dig Surg. 2020;19:1119–34.
3. SEYEDPOUR S M, NABATI M. Application of magnetic resonance imaging in liver biomechanics: A systematic review [J]. Front Physiol. 2021;12:733393.
4. Jiang J, Li J, Chu Z, et al. In vivo multiparametric magnetic resonance imaging study for differentiating the severity of hepatic warm ischemia-reperfusion injury in a rabbit model. Magn Reson Imaging. 2020;74:105–12.
5. Ji Q, Chu ZQ, Ren T, et al. Multiparametric functional magnetic resonance imaging for evaluation of hepatic warm ischemia-reperfusion injury in a rabbit model. BMC Gastroenterol. 2017;17:161.
6. Li J, Jiang J, Chu Z, et al. Multiparametric MRI evaluation of liposomal prostaglandins E1 intervention on hepatic warm Ischemia-Reperfusion injury in rabbits. J Magn Reson Imaging JMRI. 2020;52:217–28.
7. Yablonskiy DA, Sukstanskii AL, He X. Blood oxygenation level-dependent (BOLD)-based techniques for the quantification of brain hemodynamic and metabolic properties - theoretical models and experimental approaches. NMR Biomed. 2013;26:963–86.
8. Wengler K, Wang J, Serrano Sosa M, et al. Mapping hepatic blood oxygenation by quantitative BOLD (qBOLD) MRI. Magn Reson Med. 2019;81:3272–82.
9. MERGENTAL CLARKEG. How machine perfusion ameliorates hepatic ischaemia reperfusion injury. Int J Mol Sci. 2021;22:7523.
10. TAHA M A I, BADAWY M E I, ABDEL-RAZIK R K, et al. Mitochondrial dysfunction and oxidative stress in liver of male albino rats after exposing to sub-chronic intoxication of Chlorpyrifos, Cypermethrin, and Imidacloprid [J]. Pestic Biochem Physiol. 2021;178:104938.
11. MALIK I A AMANZADAA, NISCHWITZ M, et al. Myeloperoxidase and elastase are only expressed by neutrophils in normal and in inflamed liver. Histochem Cell Biol. 2011;135:305–15.
12. SIRAKI A G. The many roles of myeloperoxidase: from inflammation and immunity to biomarkers, drug metabolism and drug discovery. Redox Biol. 2021;46:102109.
13. LI R, YANG W, YIN Y, et al. 4-OI attenuates carbon Tetrachloride-Induced hepatic injury via regulating oxidative stress and the inflammatory response. Front Pharmacol. 2021;12:651444.
14. VAN RIEL W G, VAN GOLEN R F, REINIERS M J, et al. How much ischemia can the liver tolerate during resection? Hepatobiliary Surg Nutr. 2016;5:58–71.
15. XIAO L, XIAO E. Blood oxygen level-dependent functional magnetic resonance imaging can evaluate the efficiency of transcatheter arterial chemoembolization in hepatocellular carcinoma. J Interv Med. 2019;2:5–7.
16. Ji Q, Shen W, Chu ZQ, et al. Hepatic venous congestion after living donor liver Transplantation:Multi-slice spiral CT perfusion study. J Practical Radiol. 2010;26:673–7.
17. Wood JC, Cohen AR, Pressel SL, et al. TWiTCH investigators. Organ iron accumulation in chronically transfused children with sickle cell anaemia: baseline results from the twitch trial. Br J Haematol. 2016;172:122–30.

Publisher's note